PRIMARY RESEARCH ARTICLE

WILEY Global Change Biology

Carbon flux from decomposing wood and its dependency on temperature, wood N$_2$ fixation rate, moisture and fungal composition in a Norway spruce forest

Katja T. Rinne-Garmston [ID] | Krista Peltoniemi | Janet Chen [ID] | Mikko Peltoniemi | Hannu Fritze | Raisa Mäkipää

Natural Resources Institute Finland (Luke), Helsinki, Finland

Correspondence
Katja T. Rinne-Garmston, Natural Resources Institute Finland (Luke), Helsinki, Finland.
Email: katja.rinne-garmston@luke.fi

Abstract

Globally 40–70 Pg of carbon (C) are stored in coarse woody debris on the forest floor. Climate change may reduce the function of this stock as a C sink in the future due to increasing temperature. However, current knowledge on the drivers of wood decomposition is inadequate for detailed predictions. To define the factors that control wood respiration rate of Norway spruce and to produce a model that adequately describes the decomposition process of this species as a function of time, we used an unprecedentedly diverse analytical approach, which included measurements of respiration, fungal community sequencing, N$_2$ fixation rate, *nifH* copy number, ^{14}C-dating as well as N%, δ^{13}C and C% values of wood. Our results suggest that climate change will accelerate C flux from deadwood in boreal conditions, due to the observed strong temperature dependency of deadwood respiration. At the research site, the annual C flux from deadwood would increase by 27% from the current 117 g C/kg wood with the projected climate warming (RCP4.5). The second most important control on respiration rate was the stage of wood decomposition; at early stages of decomposition low nitrogen content and low wood moisture limited fungal activity while reduced wood resource quality decreased the respiration rate at the final stages of decomposition. Wood decomposition process was best described by a Sigmoidal model, where after 116 years of wood decomposition mass loss of 95% was reached. Our results on deadwood decomposition are important for C budget calculations in ecosystem and climate change models. We observed for the first time that the temperature dependency of N$_2$ fixation, which has a major role at providing N for wood-inhabiting fungi, was not constant but varied between wood density classes due to source supply and wood quality. This has significant consequences on projecting N$_2$ fixation rates for deadwood in changing climate.

KEYWORDS
activation energy, boreal forest, carbon flux, coarse woody debris, N$_2$ fixation, *nifH*, respiration rate, wood-inhabiting fungi

1 | INTRODUCTION

Decomposition of deadwood releases globally billions of tons of carbon (C) per year to the atmosphere (Harmon, Krankina, Yatskov, & Matthews, 2001), a magnitude that is similar to the emissions from fossil fuel combustion (Le Quéré et al., 2013). However, the current estimate is based on an incomplete knowledge of drivers of wood decomposition and their relation to ambient conditions, such as temperature and soil moisture, which are likely to change in the future. Consequently, it is important to quantify the factors that control respiration rates and to determine the pattern and magnitude of C flux rates at different stages of decomposition, so that the contribution of this C stock to total ecosystem respiration can be adequately accounted for in ecosystem, C accounting and climate change models.

The dynamics of wood respiration are still relatively poorly understood in comparison to other fluxes of forest respiration (Liu, Schaefer, Qiao, & Liu, 2013). Firstly, the published models describing wood decomposition have substantial differences: they predict different temporal patterns of decomposition and highly variable residence times for deadwood of the same tree species on forest floor (Harmon et al., 1986). The negative exponential model, which is one of the most commonly used to estimate wood decomposition, predicts fastest decomposition rate for Norway spruce at the beginning of decomposition and a long total decomposition time (>100 years; Melin, Petersson, & Nordfjell, 2009 and references therein). In contrast, for the same tree species, the multiple-exponential model of Mäkinen, Hynynen, Siitonen, and Sievänen (2006) predicts a slow decomposition rate for the first couple of decades followed by a fast rate of decomposition, which leads to 100% mass loss 60 years after death. Secondly, it has been proven difficult to disentangle the relative importance of the different factors driving decomposition. For example, according to some studies temperature and wood moisture content are the dominant factors influencing decomposition rates via their impact on microbial activity (Olajuyigbe, Tobin, & Nieuwenhuis, 2012; Wang, Bond-Lamberty, & Gower, 2002), while other studies have reported that these variables explain small portions of total variance in decomposition rate (Bradford et al., 2014; Yang et al., 2016). Other factors reported to affect the decomposition process include substrate quality (e.g. concentration of slowly decomposing lignin) (Mackensen & Bauhus, 2003; Tuomi, Laiho, Repo, & Liski, 2011), wood nitrogen (N) content (Weedon et al., 2009), soil macrofauna (Jacobs & Work, 2012) and fungal diversity (Valentin et al., 2014) and community structure (Rayner & Boddy, 1988).

Although community structure of wood-inhabiting fungi has been linked in several studies to decomposition rate of deadwood, the actual affiliated mechanisms are still poorly understood (Rajala, Peltoniemi, Pennanen, & Makipaa, 2012). One of the controlling factors is likely the succession of the fungal communities along which also physical and chemical properties of wood change. The successional change in fungal community of boreal forests generally follows a temporal pattern, initiated by the relatively inefficient soft-rot fungi, followed by brown-rot fungi and then by white-rot fungi, which have the unique capability to efficiently decompose wood lignin (Hyde & Jones, 2002; Rajala, Peltoniemi, Hantula, Mäkipää, & Pennanen, 2011). Finally, in boreal forests, wood becomes dominated by ectomycorrhizal (ECM) fungi, which transport N and C between soil and host plants, at the last stages of decomposition (Mäkipää et al., 2017). In addition, bacteria are considered to play a minor role in wood decomposition (Clausen, 1996), but recent studies have proven early hypothesis (Cowling & Merrill, 1966) that e.g. N_2 fixing bacteria may have a remarkable contribution on N availability in the decomposing wood (Rinne et al., 2017).

Little is still known about how different fungal species present in deadwood influence wood decomposition rate (Hoppe et al., 2016; Valmaseda, Almendros, & Martínez, 1990). Another factor that has been linked to decomposition rate, however with significant controversy, is fungal richness, measured with DNA based methods as a number of operational taxonomic unit (OTU). Some studies have reported a positive relationship between the two variables at the early to mid-stages of decomposition (Valentin et al., 2014), which has been explained by the positive impact the higher diversity of produced fungal enzymes with increasing number of OTUs has on communities' wood decomposition efficiency (Gessner et al., 2010). However, other studies have found a negative relationship between decomposition rate and OTU richness (Lindner et al., 2011; Yang et al., 2016) or no relationship at all (Hoppe et al., 2016). Other significant factors that have been reported to affect decomposition rates are competition scenarios between fungi (Renvall, 1995) and the mutualistic relationship between fungi and N_2 fixing diazotrophs (Hoppe et al., 2014).

Apart from being a substantial stock of terrestrial C, deadwood is an important component of nutrient cycling (Laiho & Prescott, 2004). This includes N, which accumulates in deadwood during the decomposition process mainly via asymbiotic N fixation (Rinne et al., 2017). N may also be used during the decomposition process via sporocarp and spore production or lost via wood fragmentation and leaching. Since saprotrophic fungi grow in wood with a very high C:N ratio and since they are at the same time highly dependent on the availability of N for production of fungal material (Moore, Gange, Gange, & Boddy, 2008), it has been suggested that there may exist a significant mutualistic relationship between N_2-fixing bacteria and wood decay fungi (Cowling & Merrill, 1966; Mäkipää et al., 2018). The first evidence of this was seen in the study of Hoppe et al. (2014), who reported a positive correlation between the number of fungal fruiting bodies and a nitrogenase-related gene, *nifH*, diversity. How well *nifH* distribution in decomposing wood relates to actual N_2-fixation and respiration rates are yet to be determined. Furthermore, fungal fruit bodies, as used in the study of Hoppe et al. (2014), may not be representative of the fungal community present in deadwood (Hoppe et al., 2016), and hence fungal community sequencing could provide additional information on the associations between diazotrophs and wood-habiting fungi.

Both respiration and N_2 fixation rates of fallen deadwood may increase as ambient temperature increases due to ongoing climate change, if wood moisture does not become limiting (too low or too high). Hence, climate warming may have significant consequences for the role of deadwood as a long-term C reservoir and on the availability of N in acutely nutrient-limited high latitude forest ecosystems. The metabolic theory of ecology (MTE) (Brown, Gillooly, Allen, Savage, & West, 2004) argues that the impact of climate warming on the decomposition and N_2 fixation rates of deadwood can be predicted from the temperature dependencies of the corresponding biochemical reactions, respiration and N_2 fixation, respectively. The temperature sensitivity of these reactions are quantified by the activation energy (AE) (Arrhenius, 1915), with a canonical value of 2.18 eV for the nitrogenase enzyme (Ceuterick, Peeters, Heremans, Smedt, & Olbrechts, 1978) and of 0.60–0.70 eV for respiration (Allen, Gilloolz, & Brown, 2005), for the temperature ranges 0°C–22°C and 0°C–30°C, respectively. However, the MTE does not take into account limitations and temperature induced changes in resource supply, which may lead to AEs that diverge from the canonical value. For example, Welter et al. (2015) reported that stream biofilm development in Iceland, amplified temperature response of respiration owing to increased N supply, which was the result of increased temperature. Conversely, Follstad Shah et al. (2017), who used data from 169 published studies, concluded that litter decomposition rates had AEs that were approximately half the value predicted by metabolic theory due to limitations for example in litter supply regime, litter quality and detritivore density. For deadwood a similar study on the AE of respiration and N_2 fixation has not been conducted to the best of our knowledge.

This study was conducted on deadwood of Norway spruce (*Picea abies* (L.) Karst.) to define the factors that control wood decomposition rates at different stages of decomposition and to resolve the debated question on the type of model that best describes the decomposition process of this species as a function of time. Furthermore, we used this knowledge to obtain estimates of annual CO_2 production rates from deadwood in current conditions and as a result of projected climate warming. To achieve our goals we used an unprecedentedly diverse dataset, which included measurements of respiration, fungal community sequencing, N_2 fixation rate, *nifH* copy number, ^{14}C-dating as well as N content, $\delta^{13}C$ and C% values of wood.

2 | MATERIALS AND METHODS

2.1 | Site description and fieldwork

Fieldwork was carried out at the Lapinjärvi forest located in southern Finland (60°66N, 26°12E). It is an unmanaged site, with a living Norway spruce trees biomass of 119,000 kg/ha (296 m³/ha) that constitutes 72% of all tree species (Rajala et al., 2012). The biomass of spruce deadwood, which accounts for 89.4% of all deadwood, is shown in Table 1 for each decay class, as classified by the system of

Harmon and Sexton (1996). Two 5 cm thick disks were obtained from 49 decomposing logs. The collected disks were evenly distributed between the five decay classes (Mäkipää et al., 2018). The disks were packed into plastic bags and stored within the same day in a freezer at −20°C until processed. Under natural forest floor conditions logs experience freeze-thaw -cycles annually, so the storage method was not considered to have an unnatural impact on the analytical results. Wood density was determined for each log as described in Rajala et al. (2012) using one of the two obtained discs. Details of the density classification (Table 1) are given in Rinne et al. (2017) and in Supporting Information S1. In addition, seven living Norway spruce trees were sampled to the pith using an increment borer for determining the initial wood C%.

2.2 | Meteorological data

A 2-year record of average daily temperature measured with data loggers at 1 m above ground level in Ruotsinpyhtää forest was used. The forest, which is located 18 km from the Lapinjärvi forest, has a similar tree composition (spruce dominated, tree density), mean annual temperature (4.6°C) and annual precipitation (618 mm) as Lapinjärvi.

2.3 | Incubation and gas chromatography (GC) analysis

Each of the thawed disks was chopped into wood chips and divided into eight equal subsamples that were placed into 118 ml bottles with an air tight cap and the fresh weight was recorded. Seven of the bottles were used for CO_2 measurements and one was reserved for other analyses (molecular and isotope analyses). First, all eight bottles were preincubated for 1 week at 14.5°C. Subsequently, the seven bottles reserved for gas chromatography were incubated 5 days at different temperatures (8.7°C, 14.5°C, 20.5°C, 26°C, 30°C, 34°C and 40.1°C) and the additional eighth bottle reserved for other analyses was incubated at 14.5°C. Samples were incubated under stable conditions by controlling the moisture content (replacement of evaporated water) and aerating the bottles (30 s per aeration) during the preincubation and incubation periods. The samples that were reserved for analyses other than GC (molecular and isotope analyses) were frozen and freeze-dried following the incubation period.

For the incubated samples respiration rates were determined by sampling the headspace of a bottle and analysing the amount of CO_2 using a gas chromatogram (Smolander, Kitunen, Tamminen, & Kukkola, 2010). The bottles were aerated 24 hr before sampling. Finally, samples were dried in an oven at 60°C for 48 hr and the dry mass was calculated for each sample.

2.4 | Molecular and bioinformatics analyses

The 49 freeze-dried samples were milled to fine particle size to ensure homogeneity for molecular and isotope analysis. Details about

TABLE 1 Deadwood characteristics of Norway spruce from the Lapinjärvi forest

	Density class				
	I (n = 10)	II (n = 7)	III (n = 8)	IV (n = 13)	V (n = 11)
Activation energy of N_2 fixation (eV)	0.69	0.60	1.27	1.04	0.40
Activation energy of respiration (eV)	0.68	0.63	0.63	0.59	0.61
Biomass of deadwood (kg/ha)	8,641	9,214	3,011	3,982	427
C in deadwood (kg C/ha)	4,051	4,394	1,412	1726	231
Fungal Shannon index	2.3 ± 1.0	2.5 ± 1.5	2.9 ± 0.9	3.5 ± 0.5	3.6 ± 0.4
Moisture (%)[a]	29 ± 6	39 ± 11	61 ± 14	78 ± 5	79 ± 3
nifH copies/g	$1.17 \times 10^7 ± 1.35 \times 10^7$	$3.89 \times 10^7 ± 4.17 \times 10^7$	$4.16 \times 10^8 ± 6.71 \times 10^8$	$1.22 \times 10^9 ± 8.39 \times 10^8$	$6.54 \times 10^8 ± 3.93 \times 10^8$
Wood absolute N content (kg N/m^3)	0.251 ± 0.025	0.249 ± 0.053	0.283 ± 0.134	0.355 ± 0.143	0.516 ± 0.112
Wood $\delta^{13}C$ (‰)	−24.48 ± 0.60	−25.20 ± 0.92	−25.63 ± 0.50	−25.35 ± 0.75	−26.24 ± 0.85
Wood density (kg/m^3)	380 ± 30	310 ± 20	240 ± 30	180 ± 20	140 ± 10
Wood C content (%)	50.8 ± 1.4	52.4 ± 1.3	53.5 ± 1.4	52.7 ± 3.7	56.0 ± 2.5

[a]Rinne et al. (2017).

DNA extraction, fungal internal transcribed spacer (ITS) sequencing procedure with Illumina platforms as well bioinformatics for the obtained fungal ITS data are described in Supporting Information S2. Shannon diversity indices from fungal ITS data were obtained by using the summary.single command in the MOTHUR software package v.1.3.6 (Schloss et al., 2009). Venn diagrams were constructed to view unique and shared fungal OTUs in wood density classes by using the venn() command implemented in library gplots in R package version 3.2.2 .

To detect the copy numbers of N_2-fixing bacteria, we conducted quantitative PCR (qPCR) targeting the *nifH* gene with PolF forward and PolR reverse primers (Poly, Monrozier, & Bally, 2001). First standard curves were constructed with plasmids containing corresponding inserts, taking into account the molecular mass of the plasmid, including the insert, and the plasmid concentration. We ran qPCR (Rotor-Gene 6000; QIAGEN, The Netherlands) with Maxima™SYBR Green qPCR Master Mix (2×) (Thermo Fisher Scientific, Germany) in a 20 ml final reaction volume containing 1 µl template, 0.3 mM of each primer and 1× qPCR master mix. Fluorescence was measured at the end of each extension step. Each qPCR run was carried out under the following conditions: initial denaturation at 95°C for 10 min, 40 cycles denaturation at 95°C for 15 s, annealing at 55°C for 30 s and extension at 72°C for 30 s, and final extension at 72°C for 10 min and from 60°C to 99°C (ramp: 1°C per 5 s). All samples were replicated and lack of PCR inhibition was verified through 1:10 dilution. The copy numbers in samples were calculated based on comparison to threshold cycle values of the standard curve and are given per gram of soil (dry weight).

2.5 | Stable isotope analysis

The 49 freeze-dried and milled deadwood samples were weighed into tin capsules for C% and $\delta^{13}C$ measurements in an elemental analyser (EA; Costech 4010; Costech Analytical Technologies Inc., Valencia, CA, USA) connected in continuous-flow mode to an
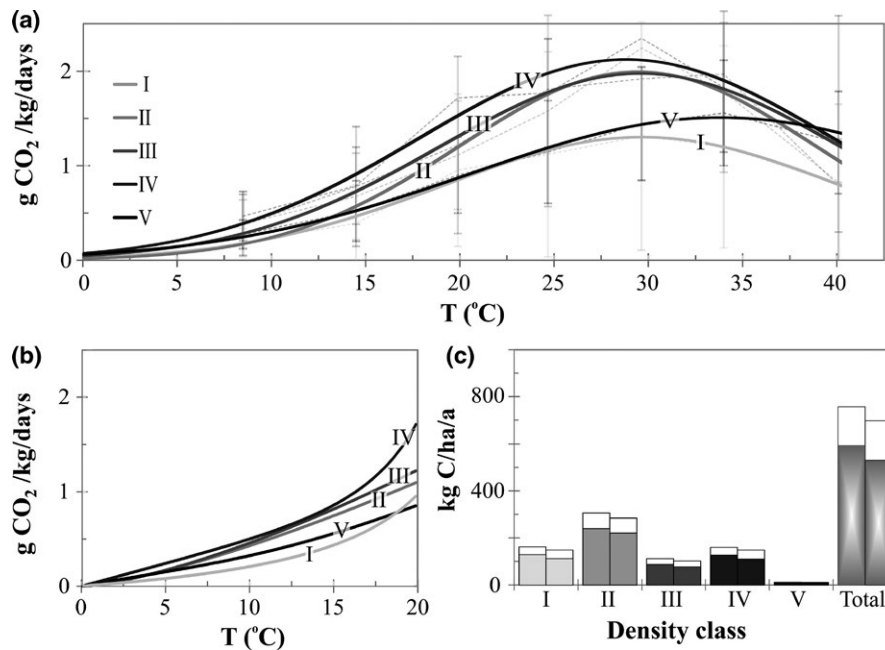
FIGURE 1 CO_2 production and C flux of Lapinjärvi deadwood. (a) The measured respiration rates (dotted lines) and their standard deviation for each incubation temperature are shown for each density class. For each series the best-fit trendline (Gaussian, $p < 0.001$) is given (bold lines) (r-values: I = 0.45, II = 0.63, III = 0.55, IV = 0.62 and V = 0.72. (b) The best-fit trendlines for the data that cover the temperature range 8.7°C–19.9°C only (I: saturation growth rate, II and III: power, IV: Farazdaghi-Harris-YD, V: polynomial regression). (c) The estimated annual levels of C flux of fallen spruce logs in Lapinjärvi. The results are shown separately for each of five density classes and for the years 2007 (left bar of a pair of bars) and 2008 (right bar of a pair of bars). The total CO_2 production is also indicated. The white bars indicate the estimated increase in respiration rate for the time period 2040–2069 under the climate warming scenario RCP 4.5, when assuming that the store of downed deadwood does not change in time (Ruosteenoja et al., 2013)

isotope ratio mass spectrometer (IRMS; Finnigan Delta Plus XP; Thermo Fisher Scientific, Waltham, MA, USA). The standard deviations for repeated analyses of reference materials were better than 0.2‰. The isotope signature is expressed in the delta notation $\delta^{13}C = (R_{sample}/R_{standard} − 1) × 1,000$ (‰) relative to the international standard VPDB, where $R = {}^{13}C/{}^{12}C$ of the sample or standard.

2.6 | N_2 fixation rate

The N_2 fixation rate of Lapinjärvi deadwood and its dependency on density class and ambient temperature has been published in Rinne et al. (2017), where the methodology is described in detail. In short, an acetylene reduction assay (ARA) was performed following Leppänen, Salemaa, Smolander, Mäkipää, and Tiirola (2013). After 24 hr of incubation the concentration of ethylene in the headspace was analysed by a gas chromatograph. A conversion factor from acetylene reduction to N fixation of 4 was used (Brunner & Kimmins, 2003). In the present study the N_2 fixation data (Rinne et al., 2017) is for the first time compared with respiration rate, *nifH* copy number and fungal community of Lapinjärvi deadwood, and used to calculate the AE of the N_2 fixation rate for the different decay classes. The density, N content and moisture of deadwood used in the present study (Table 1) are from Rinne et al. (2017).

2.7 | Activation energies

Activation energies were estimated individually for respiration and N_2 fixation using the Van't Hoff-Arrhenius relationship $e^{−E/(kT)}$, where E is the AR (in eV), k is the Boltzmann constant ($8.61 × 10^{−5}$ eV/K, 1 eV = 96.485 kJ/mol) and T is temperature (K, here the incubation temperature) (Arrhenius, 1889). For each density class the data were plotted separately in a xy-diagram, where x was $1/(kT)$ and y was the natural logarithm of each respiration or N_2 fixation measurement. Linear least-squares regression was used to describe the relationship between the variables. The AE is the absolute value of each slope.

2.8 | Statistical analysis

CurveExpert 1.4 software package was used to determine the best-fitting trendlines for the respiration series. When obtaining best-fit trendlines for the part of the respiration dataset that covered only the temperature range typical for the study area (<20°C, Figure 1b), it was necessary to add data points that approximated zero values for both CO_2 production rate and temperature (0.001 g CO_2 $kg^{−1}$ $day^{−1}$ and 0.001°C, respectively) for the trendline fitting process. With this addition the resulting best-fit trendlines did not predict a significant production of CO_2 at 0°C. The number of these added data points equalled to the number of samples
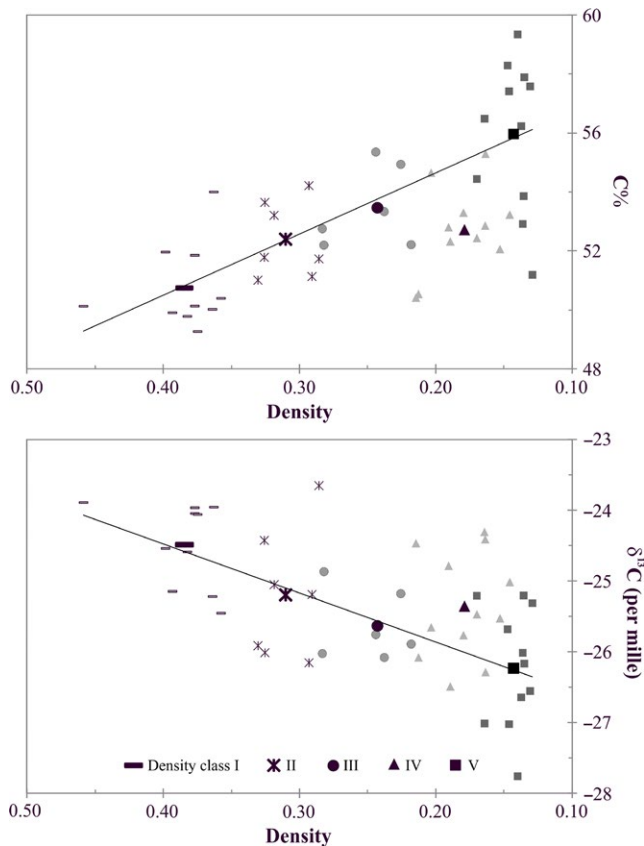
FIGURE 2 C% and δ^{13}C measurements of Lapinjärvi deadwood with respect to density. The distribution of the samples into five density classes is shown. Large symbols show means of each density classes. The linear trendlines, based on density classes I, II, III and V, are given for C% (R^2 = 0.58) and δ^{13}C (R^2 = 0.49) [Colour figure can be viewed at wileyonlinelibrary.com]

incubated at 8.8°C for each density class (n_I = 10, n_{II} = 7, n_{III} = 8, n_{IV} = 11 and n_V = 11).

IBM SPSS Statistics 22 software package (IBM Corp, Armonk, NY, USA) was used for other statistical analysis: ANOVA and ANCOVA with the Tukey post-hoc test were used to determine any significant differences between the means of groups, and simple linear and multiple regression analyses were used to study the relationship between two or more variables.

2.9 | The total amount of C stored in Lapinjärvi deadwood and its annual C flux

Annual CO_2 production per hectare (kg C ha^{-1} year^{-1}, Figure 1c) was estimated for Lapinjärvi deadwood using the trendlines of Figure 1b, the weight of wood per hectare calculated for each decay class ("log density" in Table 1) and the meteorological data. The total annual level of C flux per gram of Lapinjärvi deadwood (g C kg^{-1} year^{-1}) was calculated by dividing the density class specific results of Figure 1c by the density of fallen spruce logs in each density class (Table 1) and by summing the results. The total amount of C stored in Norway spruce deadwood in the study site was calculated for each density

class (Table 1) using the C content (Figure 2), the density of each deadwood sample (Rinne et al., 2017) and the quantity of downed dead trees (Table 1).

2.10 | Climate warming scenario RCP 4.5

The potential impact of climate warming on CO_2 production rates was calculated using the RCP4.5 temperature scenario, which assumes that a further increase in anthropogenic CO_2 production rate is followed by a decrease starting around year 2040, for the time period 2040–2069 for southern Finland (Ruosteenoja, Räisänen, & Jylhä, 2013). The projected temperature increase is approximately 1.4°C for the summer months and increasingly higher towards the winter months, where up to 3.8°C increase is estimated.

3 | RESULTS

3.1 | Respiration

For each density class the statistically significant temperature dependency of CO_2 production followed the Gaussian model, where maxima was at 29.6°C (for wood in density class I–IV) or at 34.0°C (density class V) incubation temperature (Figure 1a). According to the Gaussian model, ambient temperature explained 20% (class I), 40% (II), 34% (III), 38% (IV) and 52% (V) of the measured respiration rate. Decomposition rate was highest for the intermediate classes (II–IV) reaching respiration rates of up to 2.4 g CO_2 kg^{-1} day^{-1}. When temperature was included as covariate, there was a statistically significant difference in mean decomposition rates for density classes I and III, I and IV and IV and V (see Supporting Information S3).

Increased wood moisture significantly increased respiration at early stages of decomposition, whereas N content had the strongest impact on respiration rate for class II–IV wood (Table 2). The rate of N_2 fixation, on the other hand, did not correlate with respiration rate. No significant correlations were obtained for the respiration rate in comparison to δ^{13}C, C% and *nifH* copy number of deadwood.

Density class II wood, which contains the highest amount of C ("C in deadwood" in Table 1), produced annually the largest amount of CO_2 whereas the contribution of class V was minor (Figure 1c). Despite the low amount of class IV wood in the study site relative to wood at early stages of decomposition (I–II) (Table 1), this decay class is a source of a significant annual release of CO_2 to the atmosphere due to its higher rate of respiration (Figure 1c). The total annual C flux from Lapinjärvi deadwood was calculated to be on an average 566 kg C ha^{-1} year^{-1} for the 2 years (Figure 1c), which equals to 117 g C kg^{-1} year^{-1}. The potential impact of climate warming on CO_2 production rates was calculated using the RCP4.5 temperature scenario (Ruosteenoja et al., 2013). The calculated increase in the annual respiration rate for Norway spruce deadwood was 28% (Figure 1c) assuming that the deadwood quantity and distribution to density classes is similar to current stock. The total biomass and C stock of Norway spruce deadwood in the study site is shown in Table 1. It indicates that in our study site the majority of C (71%) is

TABLE 2 Correlation coefficients between CO_2 production, N_2 fixation rate and measured wood properties of deadwood. Only these wood property variables are shown that significantly correlated with CO_2 production or N_2 fixation rate are shown. "Class combination" shows the combination of density classes with the highest correlation coefficient. The sample number in correlation analysis is given. The significance levels are $p < 0.05$ (*) and $p < 0.001$ (**)

Variables	Density class					
	I ($n = 10$)	II ($n = 7$)	III ($n = 8$)	IV ($n = 13$)	V ($n = 11$)	Class combination
CO_2 versus moisture[a]	0.28	0.52	−0.51	−0.16	0.08	0.50* (I-II)
CO_2 versus N content[a]	−0.09	0.67	0.83*	0.58*	0.21	0.61** (II-IV)
CO_2 versus Shannon index	−0.33	−0.58	0.24	−0.39	−0.62*	−0.49* (IV-V)
N_2 fixation versus moisture	0.74*	0.72	0.74*	0.38	0.21	0.76** (I-III)
N_2 fixation versus nifH copies	0.37	0.35	0.55	0.19	0.57*	0.52** (I-IV)
N_2 fixation versus M2[b]						0.68** (I-IV)
nifH copies versus moisture	−0.06	0.64	0.64	0.52	0.53	0.72** (I-IV)
nifH copies versus N content	0.27	0.01	0.18	−0.10	−0.65*	
nifH copies versus Shannon index	−0.03	0.29	0.51	0.22	0.39	0.43** (I-V)

[a]Moisture, N content and N_2 fixation rate data were obtained from Rinne et al. (2017). [b]Multivariate analysis 2; independent variables: moisture, N content and nifH copy number.

stored in wood that is at its early stages of decomposition (I–II) of which density class I (represents 34% of deadwood C stock) is least sensitive to temperature.

To produce the best possible estimates of annual respiration rates for deadwood at the study site, best-fit trendlines were separately defined by decay class for the CO_2 data covering the temperature range typically encountered in Finland (average day temperature <20°C) (Figure 1b). The best-fit trendlines (Figure 1b, CurveExpert 1.4) were a significantly better fit than the Gaussian trendlines of Figure 1a for the measured data at the temperature range 0–10°C. The annual respiration rate of deadwood was calculated for each density class using the trendlines of Figure 1b and the temperature data representing the Lapinjärvi forest (Figure 3a). The rate of respiration with advancing stage of decomposition is best explained by a quadratic fit trendline (Figure 3a, CurveExpert 1.4). Using the temporal ^{14}C-dating based decomposition model established for our study site (figure 6a in Rinne et al., 2017), it was possible to define the dependence of respiration rate (g C kg^{-1} $year^{-1}$) on the time of decomposition since soil contact (years) as shown in Supporting Information S4. This dependency (equation in Supporting Information S4) was then used to calculate the decomposition of the current biomass of deadwood (Table 1) as a function of time (Figure 3b). According to Figure 3b, after 60 years of decomposition (the time it takes for class I wood to decompose to class V wood), 24% of the current biomass of deadwood still remains on the forest floor of the study site. For class I wood, with the approximate age of 8 years (Rinne et al., 2017), wood content was calculated also for the preceding 7 years using the established decomposition model. Consequently, it was possible to determine the trendline that best describes wood decomposition during the first 69 years of decomposition (Sigmoidal model:

$y = (ab + cx^d)/(b + x^d)$, $r = 1.00$) ("Wood decomposition model" in Figure 3b). When the first 7 years of decomposition are excluded, the decomposition is well-described by negative exponential trendline ($r = 1.00$). Based on the Sigmoidal model, mass loss of 95% is reached after 116 years. The decomposition of Norway spruce as modelled in Mäkinen et al. (2006) is shown in Figure 3b for comparison (secondary y-axis: "remaining fraction"). It clearly differs from the decomposition pattern observed in the present study: (a) the decomposition rate in Mäkinen et al. (2006) is relatively slow for the first 20–30 years of decomposition (classes I–III/IV in this study), whereas in the present study decomposition rate was at maximum for class II–IV wood and (b) according to Mäkinen et al. (2006) logs disappear in much shorter time than can be expected based on the negative exponential decomposition of wood in the present study.

3.2 | Diazotrophic activity

The number of nifH copies was low in early stages of wood decomposition (I–II) but then significantly increased with advancing decomposition culminating at class IV (Figure 4, Table 1). The number of nifH copies peaked in communities associated with density class IV (Supporting Information S5). Wood moisture (Table 1) explained 52% ($p < 0.01$) of the nifH copy number for class I–IV wood. The inclusion of class V wood decreased the correlation, because of the opposite trends in nifH and moisture contents of wood (Table 1, Figure 4).

For the samples incubated at 14.5°C, which represents a typical summer temperature in the study region, (i.e. the temperature that was used for all analysis in the present study), N_2 fixation rate in classes I–IV was best explained (Table 2, $F_{3,34} = 9.850$, $p < 0.001$) by the combined impact of wood nifH gene number, moisture and N
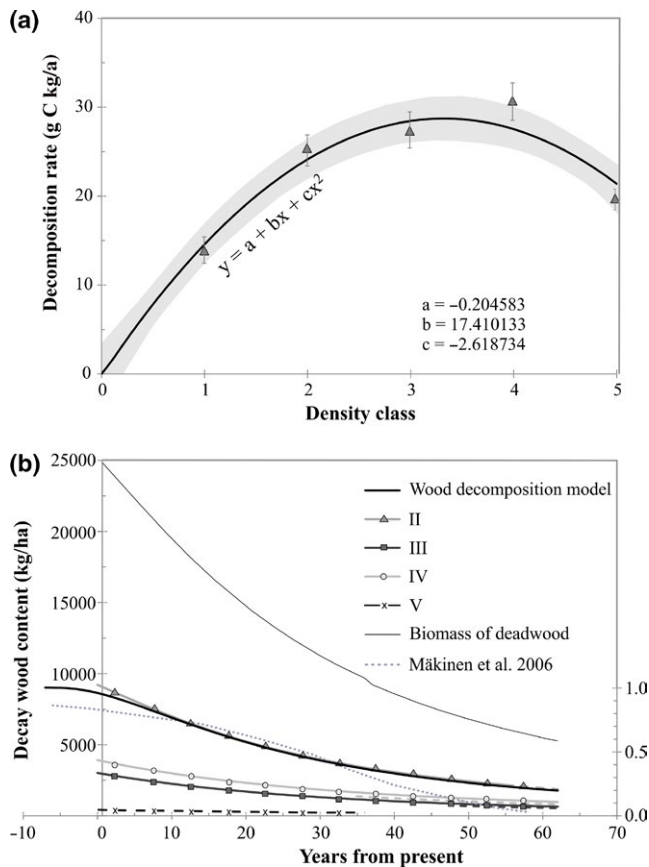
FIGURE 3 Decomposition of Lapinjärvi deadwood. (a) Annual decomposition rate of deadwood with advancing stage of decomposition. The bars indicate the standard deviation of measurement for each density class. The amount of carbon released in the decomposition process per kilograms of deadwood per year is best explained by a quadratic fit trendline (continuous line, CurveExpert 1.4). The shaded area indicates the 95% confidence level. (b) The decomposition of the current deadwood stock in the Lapinjärvi forest as a function of time until 62 years from present, which is the time it takes for class I wood (age: 8 years) to decompose to class V (age: 69 years) wood (Rinne et al., 2017). For class II–V wood it was thus necessary to forecast the decomposition model (a) beyond the age of class V wood (dashed lines). The secondary y-axis shows the remaining fraction of deadwood for the "Wood decomposition model" of the present study and for the decomposition model of Mäkinen et al. (2006) [Colour figure can be viewed at wileyonlinelibrary.com]

content. The inclusion of class V into the analysis reduced the common signal, because moisture and N content increased in wood from class IV to class V unlike N_2 fixation rate and *nifH* gene number. The N_2 fixation rate of the 49 samples were significantly dependent on the incubation temperature (Rinne et al., 2017). The density class dependency of N_2 fixation (Figure 4) resembled the density class dependency of respiration (Figure 1a) with the exception of class II, where respiration—unlike N_2 fixation—was already significantly elevated compared to the level encountered at class I.

However, the respiration and N_2 fixation rates were significantly correlated only for class IV and V wood (for 8.7°C–25.1°C: $r_{IV} = 0.41$

and $r_V = 0.42$, $p < 0.01$). For every incubation temperature, the N_2 fixation rates followed a similar trend in absolute values with advancing decomposition as the number of *nifH* copies (Figure 4). The exception was the incubation temperature 40.3°C, which had a smaller replication.

3.3 | Activation energies

The highest incubation temperatures were excluded from AE calculations (Arrhenius, 1889) (Table 3), because at temperatures above 30°C and 26°C the rate of respiration and N_2 fixation, respectively, did not increase with temperature (Figures 1 and 2). There was a strong relationship between *ln*-transformed respiration and inverse temperature for every density class (Supporting Information S6). For respiration, AE was similar at all classes and agreed with the canonical value of 0.60–0.70 (Figure 5, Table 1) (Allen et al., 2005). AEs of N_2 fixation, on the other hand, were highest for class III (1.27 eV) and IV (1.04 eV) wood but the calculated AEs were always substantially less than the AE of the nitrogenase enzyme (2.18 eV) (Figure 5, Table 1) (Ceuterick et al., 1978).

3.4 | Relationship between fungi, respiration rate and diazotrophic activity

A detailed description of the obtained fungal OTUs, their phylotypes and functional groupings from this study can be found in Rinne et al. (2017) and in Supporting Information S2. A total of 393,071 sequence reads scattered in 69 fungal phylotypes, and of these 25% could be placed into functional fungal groups according to a literature review (see Rinne et al., 2017). Of the identified phylotypes 5% were white-rot, 3% were brown-rot and 12% were mycorrhizal fungi. Over 70% of the identified white-rot fungi sequences belonged to four species: *Resinicium bicolor*, *Phellopilus nigrolimitatus*, *Exidia sp.* and *Phellinus viticola*. Almost 90% of the brown-rot fungal sequences belonged to *Antrodia serialis*, *Amyloporia sinuosa* and *Coniophora olivacea*, and over 50% of mycorrhizal fungal sequences to *Pseudotomentella tristis* and *Piloderma byssinum*. The number of fungal OTUs specific to density classes I, II, II, IV and V were 312, 104, 121, 381 and 396, respectively, and there were 482 OTUs common to all classes (Supporting Information S7). The most specific fungal phylotypes in a density class were not always the most dominant ones in a density class. For example, several typical mycorrhizal species (species of genera *Cortinarius*, *Russula*, *Piloderma*) specific to density class V were not among the most dominant ones (Supporting Information S8 and S9).

The fungal Shannon diversity index increased from class I to class V (Table 1). For all data, the index correlated with *nifH* copy number ($r = 0.43$, $p < 0.01$), moisture ($r = 0.57$, $p < 0.01$), density ($r = -0.53$, $p < 0.01$) and C% ($r = 0.37$, $p < 0.05$), but not with CO_2 production. The exception was a significant (negative) correlation between fungal diversity and respiration rate for class V wood (Table 2).
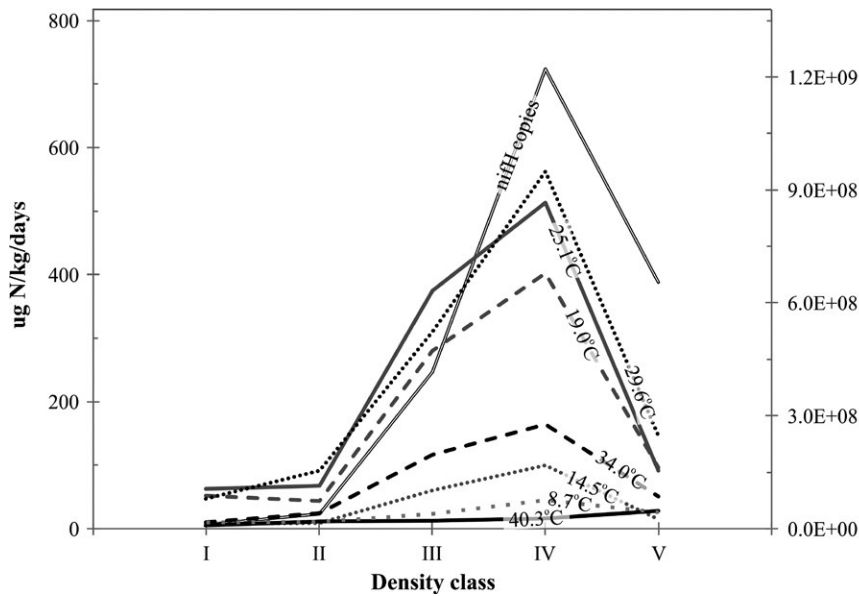
FIGURE 4 Comparison of measured N_2 fixation rates at different incubation temperatures and *nifH* gene copies per gram dry weight in Lapinjärvi deadwood at different stages of decomposition. *NifH* analysis were carried out on samples incubated at 14.5°C for Lapinjärvi deadwood at different stages of decomposition. Data points were joined with a continuous line for each series to enhance visual comparison

TABLE 3 Linear least-squares regression between *ln*-transformed respiration or N_2 fixation and inverse temperature of Norway spruce deadwood by density class. The absolute value of each slope indicates the activation energy

Measurement	Density class	R^2	P	Slope
Respiration	I	0.28	<0.001	−0.68
	II	0.49	<0.001	−0.63
	III	0.62	<0.001	−0.63
	IV	0.59	<0.001	−0.59
	V	0.64	<0.001	−0.61
N_2 fixation	I	0.30	0.001	−0.69
	II	0.27	0.021	−0.60
	III	0.50	<0.001	−1.27
	IV	0.43	<0.001	−1.04
	V	0.21	0.006	−0.40

FIGURE 6 The relative abundance of white-rot, brown-rot and ectomycorrhizal fungi in different density classes of Lapinjärvi deadwood

The relative abundance, as defined by the number of OTU reads, of white-rot, brown-rot and mycorrhizal fungi varied by density class (Figure 6). For white-rot fungi relative abundance decreased from class I to III and then peaked at class IV. The relative abundance of brown-rot fungi increased from class I (36%) to III (92%) and was relatively small in the samples of classes IV (15%) and V (13%). Mycorrhizal fungi were nearly absent in classes I–III (I: 0.0 ± 0.1%, II: 0.0 ± 0.2%, III: 0.1 ± 6%). Their relative abundance increased to 2.3 ± 26% in class IV and reached 27 ± 42% in class V.

The relative abundance of brown-rot fungi correlated negatively with *nifH* copy number ($r = −0.32$, $p < 0.05$) and positively with CO_2 production rate ($r = 0.33$, $p < 0.05$) (Table 4). The only abundance for individual species of brown-rot fungi that correlated with wood properties (such as *nifH* copy No. and $\delta^{13}C$) was *Amyloporia sinuosa*, which significantly increased with respiration (Table 4). The total abundance of white-rot fungi correlated negatively with respiration rate. However, at the species level the
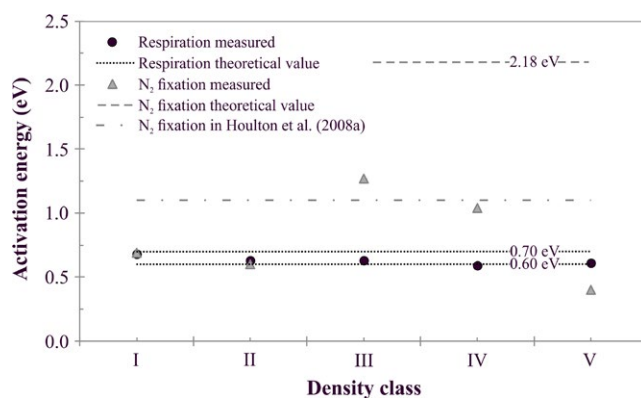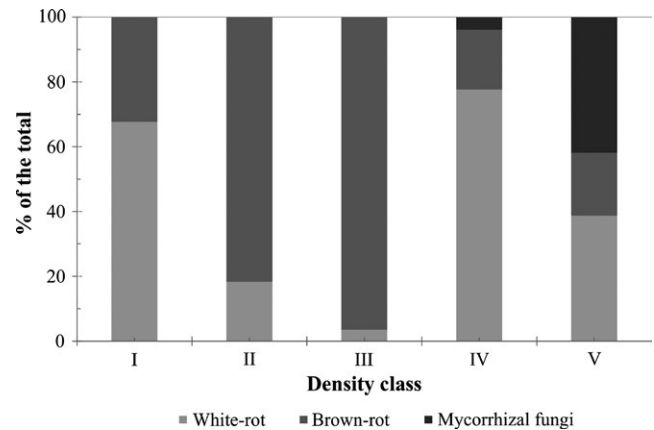

FIGURE 5 Calculated and theoretical activation energies of respiration and N_2 fixation for each density class of Lapinjärvi deadwood [Colour figure can be viewed at wileyonlinelibrary.com]

TABLE 4 Correlation coefficients between fungal abundance and deadwood properties. The *r*-values with 95% (*) and 99% (**) significance levels are shown for three functional groups (brown-rot [B], white-rot [W] and ectomycorrhizal [EC] fungi) and for those fungal species (total of ≥5,000 OTUs) that significantly correlated with the wood properties measured

	Fungi							
Wood variable	B	W	EC	*Resinicium bicolor* (W)	*Amyloporia sinuosa* (B)	*Hyphodontia alutacea* (W)	*Phellopilus nigrolimitatus* (W)	*Pseudotomentella tristis* (M)
Respiration	0.33*	−0.31*	−0.14	0.28*	0.55**	0.04	−0.26	−0.10
N$_2$ fixation	−0.21	−0.19	−0.14	−0.08	−0.04	0.07	−0.17	−0.11
nifH copy no.	−0.32*	−0.21	0.03	−0.12	−0.11	0.54**	−0.24	−0.01
C%	−0.04	−0.32*	0.38**	−0.16	−0.01	−0.02	−0.19	0.32*
δ^{13}C	−0.01	0.37*	−0.43**	0.28	−0.10	−0.17	0.34*	−0.32*

abundance of the white-rot fungi *Resinicium bicolor* correlated positively with respiration rate. Although the total abundance of white-rot fungi and *nifH* copy number did not correlate significantly in general, there was a positive correlation for class IV wood ($r_{\text{white-rotters vs. } nifH}$ = 0.58, $p < 0.05$). At the species level the abundance of white-rot fungi *Hyphodontia alutacea* correlated positively with *nifH* copy number. It should be noted, however, that these correlations have to be accepted with caution due to the DNA based approach taken in the analyses which might include fungi that are not active.

The abundance of mycorrhizal fungi did not correlate with respiration rate or diazotrophic activity but was correlated with wood C% and δ^{13}C values (positive and negative correlation, respectively, Table 4). The only relative abundance of mycorrhizal species that correlated with wood properties was that of *Pseudotomentella tristis*. Its increasing abundance was positively correlated with wood C%.

3.5 | Carbon content and δ^{13}C of deadwood

The C content (C%) and the δ^{13}C value of wood linearly increased and declined, respectively, with advancing wood decomposition with the exception of density class IV wood (Table 1, Supporting Information S3). For samples of class IV the C% values were lower (2.4%) and the δ^{13}C values more ^{13}C-enriched (0.65‰) than expected from the general trend (Figure 2).

4 | DISCUSSION

4.1 | Temperature and wood property dependency of respiration

The significant temperature and wood density class dependency of respiration (Figure 1a) clearly shows that deadwood mass loss cannot be modelled assuming constant decomposition rates throughout the decomposition process. As with many other physiological processes, rates of fungal respiration increase with an increase in temperature until the heat denatures enzymes required for growth. The generally reported general temperature limits for fungal growth (0°C–45°C) as well as the more species specific optimum temperatures for

growth (20°C–35°C) (Lacasse & Vanier, 1999) agree well with the temperature dependence of CO_2 production observed for all density classes in this study. Since the temperature optimum for fungi driven deadwood respiration is ~30°C (Figure 1a), climate warming will accelerate C loss from downed deadwood in boreal conditions in the future, unless moisture becomes limiting (too low or too high) (Figure 1c). The current mean annual C flux of 117 g C/kg measured for Norway spruce deadwood is similar to the flux reported in Forrester, Mladenoff, Gower, and Stoffel (2012) (109 and 128 g C kg^{-1} year^{-1}), who studied coarse woody debris across decay classes (CWD) in a hardwood forest in Wisconsin, USA, using instantaneous CO_2 flux measurements, and it is 30% of the C flux reported for CWD of tropical forests (Chambers, Schimel, & Bnobre, 2001). With projected climate warming the annual C flux in respiration of deadwood from the study site was calculated to increase to 149 g C/kg. However, it should be noted that this calculation does not take into account changes in total store of deadwood or in the distribution of density classes in the function of time. The current annual C flux (117 g C/kg) of deadwood accounts for 14% and 7% of the soil respiration and total ecosystem respiration (Korhonen, Pumpanen, Kolari, Juurola, & Nikinmaa, 2009), respectively. However, unlike our site in Lapinjärvi, the Scots pine dominated forest in Korhonen et al. (2009) is a managed forest, where deadwood content on forest floor is typically only <4 m^3/ha. The forest in Korhonen et al. (2009) is located 170 km northwest from our study site.

Our results do not support the conclusion of Bradford et al. (2014); that climate is not a major driver of wood decomposition rates at local scales. In our study, ambient temperature explained ~40% of the variation in respiration rate of wood that had been decomposing longer than 8 years (classes II–V, figure 1a in Bradford et al., 2014) the conclusion of the relatively low impact of temperature on respiration rate (vs. % of fungal colonization of wood) at the local scale may have been hampered by the experimental setting, where temperature was relatively constant (range of ~2°C) so that the degree for the level of fungal colonization (~2%–52%) emerged as a controlling factor at each research site. However, even Bradford et al. (2014) clearly stated that since local-scale factors–such as the availability of nitrogen and soil moisture–have a significant impact of fungal activity (Table 2), care should be

excersised when taking local results for the response of deadwood respiration rates to changes in temperature, and scaling up for use in Earth-system models.

Nevertheless, our results on temperature sensitivity of CO_2 production (and N_2 fixation) by wood density class can be implemented into models describing respiration of deadwood logs. With least effort it can be done for models describing respiration class dynamics of individual logs, which are based on the similar deadwood classification system as we used here (Peltoniemi, Penttilä, & Mäkipää, 2013). However, density class representation is not strictly required as decay class can be associated with wood density with fair accuracy (e.g. Rajala et al., 2012; this study). It is noteworthy, however, that dynamic respiration models require tying the temperature to the state variable describing the present density of decomposing matter. For one compartment model this yields a rate of mass loss $dy/dt = f(T, y) y$, where $f(T, y)$ is some continuous function representing mass loss as a function of temperature T and density y, which could be formulated based on our study and studies linking remaining mass (or density) to decay class. For more complex dynamic models, possibly representing several biochemically/physically identified compartments, implementation of aggregate temperature function requires further consideration.

Other wood properties driving respiration were increasing moisture content of wood in the early stages of decomposition (explaining 25% of respiration rate, Table 2), increasing wood N content (37%, Table 2) and the total abundance of brown-rot fungi (11%, Table 4), particularly abundance of the species *Amyloporia sinuosa* (30%, Table 4). The low level of moisture at early stages of decomposition probably explains why the temperature signal for respiration was lower for class I wood (20%, Figure 1a) than for the other decay classes (on an average 41%). Wood moisture was 35% or lower in 90% of wood samples in class I (Table 1). Wood moisture content this low has been reported to inhibit growth of fungi within wood cells (Lopez-Real & Swift, 1975). The lack of a direct dependency of respiration on wood moisture content for medium or well decomposed wood samples is in accordance with field studies, where moisture content was not limiting or excessive (Forrester et al., 2012; Herrmann & Bauhus, 2013). In contrast, in the study of Hagemann, Moroni, Gleißner, and Makeshin (2010), respiration was reduced at times by both too low and too high wood moisture content, therefore wood moisture was reported to be the dominant environmental control over CWD respiration. Similarly, for soil respiration, Reichstein et al. (2002) observed declining temperature sensitivity with increasing soil water deficit. In boreal forests with a climate similar to that of the Lapinjärvi forest, moisture may be a limiting factor only at the early stages of decomposition or for the standing dead trees (Table 2).

Our study does not support the results of Yang et al. (2016) who found that increasing fungal diversity reduced wood respiration rate. In contrast, both CO_2 production and Shannon index of fungal community increased from class I to class IV wood (Table 1). Although the respiration rate and fungal diversity both increased from class I to class IV, the two were not significantly correlated (Table 2) suggesting that high fungal diversity is not essential for enhancing respiration rate. The result is consistent with the findings of Valentin et al. (2014) who concluded that reduced biodiversity in the highly diverse fungal community of the late decay class wood did not influence rate of respiration. The divergent trend between CO_2 production rate (decrease) and fungal diversity (increase) from class IV to class V wood (Figure 1a) probably reflects the reduced wood resource quality affecting respiration rate, as opposed to any direct relationship between the two variables (Table 2). This conclusion is supported by the significant reduction in the relative abundance of saproxylic fungi in favour of mycorrhizal species from class IV to class V wood (Figure 6). Via deceleration in respiration rate, the reduced wood quality also had a negative indirect effect on N_2 fixation rate (Figure 4) by reducing the respiration rate and therefore reducing ATP production from the decomposition process that is needed as an energy source for N_2 fixation (Weißhaupt, Pritzkow, & Noll, 2011).

Our results on the density class dependency of respiration rate, where an initial slow respiration rate (density class I) was followed by rapid respiration (II–IV) and finally by a clear decline (V) at all incubation temperatures with high sample replication (8.7°C–34.0°C) (Figure 1), have clear differences compared to previous studies on conifers. Wang et al. (2002) and Wu, Zhang, Wang, Sun, and Guan (2010) studied black spruce (*Picea mariana*) and Korean pine (*Pinus koraiensis*), respectively, and reported an increase in respiration rate from the least to moderately decomposed wood but no decline for the most decomposed wood. However, their classification system for deadwood consisted of only three classes (Lambert, Lang, & Reiners, 1980). The class specific average wood densities of 0.41 g/cm³, 0.34 g/cm³ and 0.28 g/cm³ reported for black spruce (Wang et al., 2002) are similar to the densities measured for classes I, II and III of the five classes used in our study (Table 1), which suggests that well-decomposed wood was not used in the studies by Wang et al. (2002) and Wu et al. (2010). Such sampling would lead to different conclusions, when calculating models predicting mass loss due to respiration over time (Figure 3). Similarly, the study of Mäkinen et al. (2006), who modelled decomposition of Norway spruce in Finland, is based on samples that were on an average only 14 and at most 38 years old, which is significantly younger than the 62–77 years average age determined for well decomposed Norway spruce logs using ^{14}C dating (Krüger, Muhr, Hartl-Meier, Schulz, & Borken, 2014; Petrillo et al., 2015; Rinne et al., 2017). These factors may explain why the decomposition model of Mäkinen et al. (2006) is very different from the decomposition pattern observed in the present study (Figure 3b). The negative exponential decomposition model, which has been used in many studies to estimate decomposition of Norway spruce (Melin et al. (2009), is in a much better agreement with the results of the present study. However, our study indicates a clearly slower overall rate of decomposition. For example, after 60 years of decomposition the fraction of the deadwood stock remaining on forest floor is 24% in the present study and on an average ~10% according to the compilation of models in Melin

et al. (2009). This is at least partly explained by the failure of the exponential models to take into account the slow decomposition rate at the early stages of decomposition (Figures 1a and 3b). In addition, organic matter stabilization by fungi or other soil biota during the decomposition process (Chertov et al., 2017; Komarov et al., 2017) may explain slow decomposition rate of the remaining fraction in the late decay phases.

For density class II wood, respiration increased to levels comparable to those measured for class III and IV wood (Figure 1) despite the low accumulation rate of fixed atmospheric N (Figure 4), which is needed to facilitate fungal-driven decomposition. The high rate of respiration at this stage may have been enabled by soil foraging fungi that have the capability to transport soil N to wood for the production of extracellular enzymes (Allison & Vitousek, 2005; Sterner & Elser, 2002) and fungal material (Merrill & Cowling, 1966; Moore et al., 2008). 80% of the Lapinjärvi deadwood samples contained at least one species that has been reported to form mycelial cords or rhizomorphs for soil nutrient foraging (Rinne et al., 2017). The generally low N content measured for class II wood (Table 1) suggests that at this stage of decomposition there was a substantial need for N to sustain high fungal vegetative and generative growth (Hoppe et al., 2014).

4.2 | Activation energy

Due to the relatively low calculated AE of N_2 fixation of deadwood, the impact of a temperature increase on N_2 fixation rate of deadwood was smaller than expected from the temperature response of the nitrogenase enzyme (Figure 5). This is typical for high latitudes, because as temperatures decline more enzyme is needed to achieve a given rate of N_2 fixation, hence constraining maximal N_2 fixation rates (Houlton, Wang, Vitousek, & Field, 2008). However, the temperature dependency of this metabolic process was not constant for deadwood but varied according to wood supply and quality (Figure 5). For density classes I and II, low wood moisture (Table 1) reduced the temperature sensitivity of N_2 fixation (Table 2). Additionally, for class I and V wood, the low amount of ATP produced via the slow decomposition process (Figure 1) significantly limited N_2 fixation rate (Weißhaupt et al., 2011). As a consequence, the AE of N_2 fixation for class I, II and V wood (0.56 ± 0.15 eV) is significantly below the average AE of 1.1 eV reported in Houlton et al. (2008) in a unifying framework for terrestrial N_2 fixation. N_2 fixation of class III and IV wood, on the other hand, had a stronger response to increases in temperature (AE = 1.14 ± 0.18 eV). This is because wood at these stages of decomposition was not limited by wood quality and they benefited (Figure 4) from the increased production of ATP from the accelerated decomposition process (Figure 1).

The increases in N_2 fixation rates with temperature did not affect the temperature dependency of respiration at any stage of decomposition for Lapinjärvi deadwood (Figure 5). This is in contrast to the study of Welter et al. (2015), who reported 2.7-fold higher AEs of respiration than predicted by metabolic theory for biofilms in an Icelandic streamside channel due to increases in N_2 fixation with temperature. However, a major difference between our study

(Figure 5) and that of Welter et al. (2015) is that AEs calculated for biofilm N_2 fixation rates approximated the AE of the nitrogenase reaction, but that was not the case for our study (Figure 5).

4.3 | Effect of fungal community on decomposition of cellulose and lignin

The general linear relationship between wood density and wood C% as well as between wood density and $\delta^{13}C$ values mainly reflect the increasing relative abundance of lignin to cellulose (Figure 2). Cellulose, which has a lower C content (44% vs. 67%) and is from 4‰ to 6‰ more ^{13}C-enriched than lignin (Benner, Fogel, Sprague, & Hodson, 1987), is degraded at a faster rate because it is a much more energy rich resource for wood decay fungi (Moorhead & Sinsabaugh, 2006). However, eventually the remaining cellulose becomes shielded by a lignin coating, which requires enhanced activity of white-rot fungi to enable decomposition of more cellulose (Moorhead & Sinsabaugh, 2006; Rayner & Boddy, 1988). In our study, this increase in lignin breakdown seems to have occurred at density class IV, where the wood C% and $\delta^{13}C$ values are smaller and more ^{13}C-enriched, respectively, than expected from the general linear trend that they follow relative to wood density (Figure 2). This is supported by the observation that the relative abundance of white-rot fungi substantially increases from density class III to class IV, where white-rot fungi dominates the three main functional groups (Figure 6). The significant role of white-rot fungi in lignin breakdown is also indicated by the negative correlation between the abundance of this functional group in deadwood and wood C% and by the positive correlation between the abundance and wood $\delta^{13}C$ (Table 4). Since the white-rot species *H. alutacea* was specific and clearly more common to class IV (Supporting Information S8 and S9) and since its abundance correlated positively with *nifH* copy number (Table 4), it is concluded that this species had a major role in the intensified lignin decomposition at stage IV (Figure 2) that was enabled by diazotrophic N additions (Jurgensen, Larsen, Graham, & Harvey, 1987). Also, Hoppe et al. (2016) reported the dominance of *H. alutacea* in decay class IV spruce wood as well as a positive correlation between the abundance of this species and the respiration rate.

The significant breakdown of lignin at density class IV may have been enabled by the invasion of ECM fungi (Figure 6), which transfer simple sugars from trees to deadwood within their mycelia. The transfer of recent photosynthates with depleted $\delta^{13}C$ value (Rinne et al., 2015) into deadwood is supported by the significant negative correlation between the relative abundance of ECM fungi and deadwood $\delta^{13}C$ and by the positive correlation between ECM abundance and C% values (Table 4). *Pseudotomentella tristis* was a particularly important species importing labile C compounds into wood (Table 4). The invasion of wood by ECM was key factor in enabling lignin breakdown, because the consequent availability of labile C compounds in wood can function as co-metabolites in this process (Melillo et al., 1989). Furthermore, the increased availability of labile C compounds as well as the ATP generated during the faster lignin breakdown and the breakdown of the released cellulose would have benefited

diazotrophic activity leading to increased availability of N for white-rot fungi (Burgess & Lowe, 1996; Jurgensen, Larsen, Wolosiewicz, & Harvey, 1989). This mutualistic relationship between white-rotters and diazotrophs is supported by the significant correlation between the abundance of the two in class IV wood ($r_{\text{white-rotters vs. }nifH}$ = 0.58, $p < 0.05$), where both also reached their peak activity (Figures 4 and 5). The invasion of wood by ECM fungi, which increased the content of labile C compounds in wood (Mäkipää et al., 2017), at late stages of decomposition could also explain why white-rotted (further decomposed) wood has been reported to have a higher soluble sugar content than brown-rotted (less decomposed) wood in Jurgensen et al. (1989), as opposed to the hypothesised higher metabolic activity of white-rot fungi per se (Jurgensen et al., 1989). However, no data on the fungal composition of wood is available in Jurgensen et al. (1989) to evaluate this hypothesis.

In general, however, wood respiration rate was more dependent on brown-rot than on white-rot activity (Table 4). The most important species in this respect seems to be *Amyloporia sinuosa* (Table 4), which was the fifth most abundant fungi identified at species level in the studied wood samples (Supporting Information S9). The second most abundant species, the white-rot fungi *Resinicium bicolor*, was the only other identified species whose abundance correlated with the measured respiration rates. No significant correlations with respiration rate or any other measured variable were observed for *Antrodia serialis*, which was clearly the most abundant brown-rot species. As discussed by Hoppe et al. (2016), high species richness may not be associated with wood respiration rate, if a species invests more energy into competing with other species than on producing wood-degrading enzymes.

4.4 | Projecting respiration and N₂ fixation rates with climate warming

According to our results, temperature was the main, overall control on the respiration rate of deadwood in the studied Norway spruce dominated forest in Finland. This highlights the importance of adequately accounting for the effect of decomposition of coarse woody debris, which globally contains 36–72 Pg of C (Cornwell et al., 2009), on C budget calculations in forest ecosystem and climate change models. Another factor that should be accounted for in such models is the quantity of wood at different stages of decomposition on the forest floor, since respiration rate is significantly dependent on the density class of deadwood. In Finland such data on quantity of deadwood according to decomposition stages is available via the National Forest Inventories (Ihalainen & Mäkelä, 2009). Consequently, it is possible to upscale CO_2 release from coarse woody debris to regional and national levels, when density class and temperature dependency of the respiration is known. However, since decomposition rate of deadwood is also significantly dependent on local-scale factors, such as N availability and soil moisture status (Table 2), the results of the present study should not be directly applied to other sites with significantly different environmental conditions. Another major outcome of our study was that the effect of temperature

increase on N_2 fixation rate of deadwood was smaller than expected from the temperature response of nitrogenase enzyme and that the temperature dependency of this metabolic process was density class dependent, which was caused by the class specific differences in wood quality and in supply of limiting resources. The density class dependency of AE has significant consequences on projecting N_2 fixation rates for deadwood with climate warming. According to the RCP4.5 temperature scenario of Ruosteenoja et al. (2013) and the AEs observed in the present study for deadwood, by year 2040 N_2 fixation will increase ~30% for class I, II and V wood and ~60% for class III and IV wood, whereas the AE reported for terrestrial N_2 fixation by Houlton et al. (2008) would predict 158% and 50% increases, respectively.

ORCID

Katja T. Rinne-Garmston (iD) https://orcid.org/0000-0001-9793-2549

Janet Chen (iD) https://orcid.org/0000-0001-6477-4193

REFERENCES

Allen, A. P., Gilloolz, J. F., & Brown, J. H. (2005). Linking the global carbon cycle to individual metabolism. *Functional Ecology*, *19*, 202–213. https://doi.org/10.1111/j.1365-2435.2005.00952.x

Allison, S. D., & Vitousek, P. M. (2005). Responses of extracellular enzymes to simple and complex nutrient inputs. *Soil Biology and Biochemistry*, *37*, 937–944. https://doi.org/10.1016/j.soilbio.2004.09.014

Arrhenius, S. (1889). Über die Reaktionsgeschwindigkeit bei der Inversion von Rohrzucker durch Säuren. *Zeitschrift Für Physikalische Chemie*, *4*, 226–248. https://doi.org/10.1515/zpch-1889-0116

Arrhenius, S. (1915). *Quantitative laws in biological chemistry*. London, UK: Bell.

Benner, R. M., Fogel, L., Sprague, E. K., & Hodson, R. E. (1987). Depletion of ^{13}C in lignin and its implications for stable carbon isotope studies. *Nature*, *329*, 708–710. https://doi.org/10.1038/329708a0

Bradford, M. A., Warren II, R. J., Baldrian, P., Crowther, T. W., Maynard, D. S., Oldfield, E. E., ... King, J. R. (2014). Climate fails to predict wood decomposition at regional scales. *Nature Climate Change*, *4*, 625–630. https://doi.org/10.1038/nclimate2251

Brown, J. H., Gillooly, J. F., Allen, A. P., Savage, V. M., & West, G. B. (2004). Toward a metabolic theory of ecology. *Ecology*, *85*, 1771–1789. https://doi.org/10.1890/03-9000

Brunner, A., & Kimmins, J. P. (2003). Nitrogen fixation in coarse woody debris of Thuja plicata and Tsuga heterophylla forests on northern Vancouver Island. *Canadian Journal of Forest Research*, *33*, 1670–1682.

Burgess, B. K., & Lowe, D. J. (1996). Mechanism of molybdenum nitrogenase. *Chemical Reviews*, *96*, 2983–3011. https://doi.org/10.1021/cr950055x

Ceuterick, F., Peeters, J., Heremans, K., De Smedt, H., & Olbrechts, H. (1978). Effect of high pressure, detergents and phospholipase on the break in the Arrhenius plot of *Azotobacter* nitrogenase. *European Journal of Biochemistry*, 87, 401–407.

Chambers, J. Q., Schimel, J. P., & Bnobre, A. D. (2001). Respiration from coarse wood litter in central Amazon forests. *Biogeochemistry*, 52, 115–131.

Chertov, O., Komarov, A., Shaw, C., Bykhovets, S., Frolov, P., Shanin, V., … Shashkov, M. (2017). Romul_Hum-A model of soil organic matter formation coupling with soil biota activity. II. Parameterisation of the soil food web biota activity. *Ecological Modelling*, 345, 125–139. https://doi.org/10.1016/j.ecolmodel.2016.10.024

Clausen, C. A. (1996). Bacterial associations with decaying wood: A review. *International Biodeterioration and Biodegradation*, 37, 101–107. https://doi.org/10.1016/0964-8305(95)00109-3

Cornwell, W. K., Cornelissen, J. H. C., Allison, S. D., Bauhus, J., Eggleton, P., Preston, C. M., … Zanne, A. E. (2009). Plant traits and wood fates across the globe: Rotted, burned, or consumed? *Global Change Biology*, 15, 2431–2449.

Cowling, E. B., & Merrill, W. (1966). Nitrogen in wood and its role in wood deterioration. *Canadian Journal of Botany*, 44, 1539–1554. https://doi.org/10.1139/b66-167

Follstad Shah, J. J., Kominoski, J. S., Ardón, M., Dodds, W. K., Gessner, M. O., Griffiths, N. A., … Zeglin, L. H. (2017). Global synthesis of the temperature sensitivity of leaf litter breakdown in streams and rivers. *Global Change Biology*, 23, 3064–3075. https://doi.org/10.1111/gcb.13609

Forrester, J. A., Mladenoff, D. J., Gower, S. T., & Stoffel, J. L. (2012). Interactions of temperature and moisture with respiration from coarse woody debris in experimental forest canopy gaps. *Forest Ecology and Management*, 265, 124–132. https://doi.org/10.1016/j.foreco.2011.10.038

Gessner, M. O., Swan, C. M., Dang, C. K., Mckie, B. G., Bardgett, R. D., Wall, D. H., & Hättenschwiler, S. (2010). Diversity meets decomposition. *Trends in Ecology & Evolution*, 25, 372–380. https://doi.org/10.1016/j.tree.2010.01.010

Hagemann, U., Moroni, M. T., Gleißner, J., & Makeshin, F. (2010). Disturbance history influences downed woody debris and soil respiration. *Forest Ecology and Management*, 260, 1762–1772. https://doi.org/10.1016/j.foreco.2010.08.018

Harmon, M. E., Franklin, J. F., Swanson, F. J., Sollins, P., Gregory, V., Lattin, J. D., … Cummins, K. W. (1986). Ecology of coarse woody debris in temperate ecosystems. *Advances in Ecological Research*, 15, 133–302.

Harmon, M. H., Krankina, O. N., Yatskov, M., & Matthews, E. (2001). Predicting broadscale carbon stores of woody detritus from plot-level data. In R. Lal, J. M. Kimble, R. F. Follett, & B. A. Stewart (Eds.), *Assessment methods for soil carbon* (pp. 533–552). Boca Raton, FL: Lewis Publishers.

Harmon, M. E., & Sexton, J. (1996). *Guidelines for measurements of woody detritus in forest ecosystems*. Seattle, WA: University of Washington.

Herrmann, S., & Bauhus, J. (2013). Effects of moisture, temperature and decomposition stage on respirational carbon loss from coarse woody debris (CWD) of important European tree species. *Scandinavian Journal of Forest Research*, 28, 346–357. https://doi.org/10.1080/02827581.2012.747622

Hoppe, B., Kahl, T., Karasch, P., Wubet, T., Bauhus, J., Buscot, F., & Kruger, D. (2014). Network analysis reveals ecological links between N-fixing bacteria and wood-decaying fungi. *PLoS ONE*, 9, e88141. https://doi.org/10.1371/journal.pone.0088141

Hoppe, B., Purahong, W., Wubet, T., Kahl, T., Bauhus, J., Arnstadt, T., … Krüger, D. (2016). Linking molecular deadwood-inhabiting fungal diversity and community dynamics to ecosystem functions and processes in Central European forests. *Fungal Diversity*, 77, 367–379. https://doi.org/10.1007/s13225-015-0341-x

Houlton, B. Z., Wang, Y.-P., Vitousek, P. M., & Field, C. B. (2008). A unifying framework for dinitrogen fixation in the terrestrial biosphere. *Nature*, 454, 327–331. https://doi.org/10.1038/nature07028

Hyde, K. D., & Jones, E. (2002). Introduction to fungal succession. *Fungal Diversity*, 10, 1–4.

Ihalainen, A., & Mäkelä, H. (2009). Kuolleen puuston määrä Etelä- ja Pohjois-Suomessa 2004–2007. *Metsätieteen Aikakauskirja*, 1, 35–56. https://doi.org/10.14214/ma.5834

Jacobs, J. M., & Work, T. T. (2012). Linking deadwood-associated beetles and fungi with wood decomposition rates in managed black spruce forests. *Canadian Journal of Forest Research*, 42, 1477–1490.

Jurgensen, M. F., Larsen, M. J., Graham, R. T., & Harvey, A. E. (1987). Nitrogen fixation in woody residue of northern Rocky Mountain conifer forests. *Canadian Journal of Forest Research*, 17, 1283–1288. https://doi.org/10.1139/x87-198

Jurgensen, M. F., Larsen, M. J., Wolosiewicz, M., & Harvey, A. E. (1989). A comparison of dinitrogen fixation rates in wood litter decayed by white-rot and brown-rot fungi. *Plant and Soil*, 115, 117–122. https://doi.org/10.1007/BF02220701

Komarov, A., Chertov, O., Bykhovets, S., Shaw, C., Nadporozhskaya, M., Frolov, P., … Zubkova, E. (2017). Romul_Hum model of soil organic matter formation coupled with soil biota activity. I. Problem formulation, model description, and testing. *Ecological Modelling*, 345, 113–124. https://doi.org/10.1016/j.ecolmodel.2016.08.007

Korhonen, J. F. J., Pumpanen, J., Kolari, P., Juurola, E., & Nikinmaa, E. (2009). Contribution of root and rhizosphere respiration to the annual variation of carbon balance of a boreal Scots pine forest. *Biogeosciences Discussions*, 6, 6179–6203. https://doi.org/10.5194/bgd-6-6179-2009

Krüger, I., Muhr, J., Hartl-Meier, C., Schulz, C., & Borken, W. (2014). Age determination of coarse woody debris with radiocarbon analysis and dendrochronological cross-dating. *European Journal of Forest Research*, 133, 931–939. https://doi.org/10.1007/s10342-014-0810-x

Lacasse, M. A., & Vanier, D. J. (1999). *Durability of building materials and components 8*. Vancouver, BC: NRC Research Press.

Laiho, R., & Prescott, C. E. (2004). Decay and nutrient dynamics of coarse woody debris in northern coniferous forests: A synthesis. *Canadian Journal of Forest Research*, 34, 763–777. https://doi.org/10.1139/x03-241

Lambert, R. L., Lang, G. E., & Reiners, W. A. (1980). Loss of mass and chemical change in decaying boles of a subalpine balsam fir forest. *Ecology*, 61, 1460–1473. https://doi.org/10.2307/1939054

Le Quéré, C., Andres, R. j., Boden, T., Conway, T., Houghton, R. A., House, J. I., … Zeng, N. (2013). The global carbon budget 1959–2011. *Earth System Science Data*, 5, 165–185. https://doi.org/10.5194/essd-5-165-2013

Leppänen, S. M., Salemaa, M., Smolander, A., Mäkipää, R., & Tiirola, M. (2013). Nitrogen fixation and methanotrophy in forest mosses along a N deposition gradient. *Environmental and Experimental Botany*, 90, 62–69. https://doi.org/10.1016/j.envexpbot.2012.12.006

Lindner, D. L., Vasaitis, R., Kubartová, A., Allmér, J., Johannesson, H., Banik, M. T., & Stenlid, J. (2011). Initial fungal colonizer affects mass loss and fungal community development in *Picea abies* logs 6 yr after inoculation. *Fungal Ecology*, 4, 449–460. https://doi.org/10.1016/j.funeco.2011.07.001

Liu, W., Schaefer, D., Qiao, L., & Liu, X. (2013). What controls the variability of wood-decay rates? *Forest Ecology and Management*, 310, 623–631.

Lopez-Real, J. M., & Swift, M. J. (1975). Formation of pseudosclerotia ("zone lines") in wood decayed by *Armillaria mellea* and *Sterum hirsutum*. II. Formation in relation to the moisture content of wood. *Transactions of the British Mycological Society*, 64, 473–481.

Mackensen, J., & Bauhus, J. (2003). Density loss and respiration rates in coarse woody debris of *Pinus radiata*, *Eucalyptus regnans* and

Eucalyptus maculata. Soil Biology and Biochemistry, 35, 177–186. https://doi.org/10.1016/S0038-0717(02)00255-9

Mäkinen, H., Hynynen, J., Siitonen, J., & Sievänen, R. (2006). Predicting the decomposition of Scots pine, Norway spruce and birch stems in Finland. *Ecological Applications*, 16, 1865–1879. https://doi.org/10.1890/1051-0761(2006)016[1865:PTDOSP]2.0.CO;2

Mäkipää, R., Leppänen, S. M., Munoz, S. S., Somlander, A., Tiirola, M., Tuomivirta, T., & Fritze, H. (2018). Methanotrophs are core members of the diazotroph community in decaying Norway spruce logs. *Soil Biology and Biochemistry*, 120, 230–232. https://doi.org/10.1016/j.soilbio.2018.02.012

Mäkipää, R., Rajala, T., Schigel, D., Rinne, K. T., Pennanen, T., Abrego, N., & Ovaskainen, O. (2017). Interactions between soil- and dead wood-inhabiting fungal communities during the decay of Norway spruce logs. *The ISME Journal*, 11, 1–11. https://doi.org/10.1038/ismej.2017.57

Melillo, J. M., Aber, J. D., Linkins, A. E., Ricca, A., Fry, B., & Nadelhoffer, K. J. (1989). Carbon and nitrogen dynamics along the decay continuum: Plant litter to soil organic matter. *Plant and Soil*, 115, 189–198. https://doi.org/10.1007/BF02202587

Melin, Y., Petersson, H., & Nordfjell, T. (2009). Decomposition of stump and root systems of Norway spruce in Sweden – A modelling approach. *Forest Ecology and Management*, 257, 1445–1451. https://doi.org/10.1016/j.foreco.2008.12.020

Merrill, W., & Cowling, E. N. (1966). Role of nitrogen in wood deterioration: Amounts and distribution of nitrogen in tree stems. *Canadian Journal of Botany*, 44, 1555–1580. https://doi.org/10.1139/b66-168

Moore, D., Gange, A. C., Gange, E. G., & Boddy, L. (2008). Chapter 5 Fruit bodies: Their production and development in relation to environment. In J. C. F. Lynne Boddy, & W. Van Pieter (Eds.), *British Mycological Society symposia series* (pp. 79–103). New York, NY: Academic Press.

Moorhead, D. L., & Sinsabaugh, R. L. (2006). A theoretical model of litter decay and microbial interaction. *Ecological Monographs*, 76, 151–174. https://doi.org/10.1890/0012-9615(2006)076[0151:ATMOLD]2.0.CO;2

Olajuyigbe, S., Tobin, B., & Nieuwenhuis, M. (2012). Temperature and moisture effects on respiration rate of decomposing logs in a Sitka spruce plantation in Ireland. *Forestry*, 85, 485–496. https://doi.org/10.1093/forestry/CPS045

Peltoniemi, M., Penttilä, R., & Mäkipää, R. (2013). Temporal variation of polypore diversity based on modelled dead wood dynamics in managed and natural Norway spruce forests. *Forest Ecology and Management*, 310, 523–530. https://doi.org/10.1016/j.foreco.2013.08.053

Petrillo, M., Cherubini, P., Fravolini, G., Ascher, J., Schärer, M., Synal, H.-A., ... Egli, M. (2015). Time since death and decay rate constants of Norway spruce and European larch deadwood in subalpine forests determined using dendrochronology and radiocarbon dating. *Biogeosciences Discussions*, 12, 14797–14832. https://doi.org/10.5194/bgd-12-14797-2015

Poly, F., Monrozier, L. J., & Bally, R. (2001). Improvement in RFLP procedure to study the community of nitrogen fixers in soil through the diversity of nifH gene. *Research in Microbiology*, 152, 95–103.

Rajala, T., Peltoniemi, M., Hantula, J., Mäkipää, R., & Pennanen, T. (2011). RNA reveals a succession of active fungi during the decay of Norway spruce logs. *Fungal Ecology*, 4, 437–448. https://doi.org/10.1016/j.funeco.2011.05.005

Rajala, T., Peltoniemi, M., Pennanen, T., & Makipaa, R. (2012). Fungal community dynamics in relation to substrate quality of decaying Norway spruce (*Picea abies* [L.] Karst.) logs in boreal forests. *FEMS Microbiology Ecology*, 81, 494–505. https://doi.org/10.1111/j.1574-6941.2012.01376.x

Rayner, A. D. M., & Boddy, L. (1988). *Fungal decomposition of wood: Its biology and ecology*. Chichester, UK: John Wiley & Sons.

Reichstein, M., Tenhunen, J. D., Roupsard, O., Ourcival, J. M., Rambal, S., Dore, S., & Valentini, R. (2002). Ecosystem respiration in two Mediterranean evergreen Holm Oak forests: Drought effects and decomposition dynamics. *Functional Ecology*, 16, 27–39. https://doi.org/10.1046/j.0269-8463.2001.00597.x

Renvall, P. (1995). Community structure and dynamics of wood-rotting Basidiomycetes on decomposing conifer trunks in northern Finland. *Karstenia*, 35, 1–51. https://doi.org/10.29203/ka.1995.309

Rinne, K. T., Rajala, T., Peltoniemi, K., Chen, J., Smolander, A., & Mäkipää, R. (2017). Accumulation rates and sources of external nitrogen in decaying wood in a Norway spruce dominated forest. *Functional Ecology*, 31, 530–541. https://doi.org/10.1111/1365-2435.12734

Rinne, K. T., Saurer, M., Kirdyanov, A. V., Bryukhanova, M. V., Prokushkin, A. S., Churakova Sidorova, O. V., & Siegwolf, R. T. W. (2015). Examining the response of needle carbohydrates from Siberian larch trees to climate using compound-specific $\delta^{13}C$ and concentration analyses. *Plant, Cell and Environment*, 38, 2340–2352.

Ruosteenoja, K., Räisänen, J., Jylhä, K., et al. (2013). *Maailmanlaajuisiin CMIP3-malleihin perustuvia arvioita Suomen tulevasta ilmastosta*. Reports: 4. Helsinki, Finland: Finnish Meteorological Institute.

Schloss, P. D., Westcott, S. L., Ryabin, T., Hall, J. R., Hartmann, M., Hollister, E. B., ... Weber, C. F. (2009). Introducing mothur: Open-source, platform-independent, community-supported software for describing and comparing microbial communities. *Applied and Environmental Microbiology*, 75, 7537–7541. https://doi.org/10.1128/AEM.01541-09

Smolander, A., Kitunen, V., Tamminen, P., & Kukkola, M. (2010). Removal of logging residue in Norway spruce thinning stands: Long-term changes in organic layer properties. *Soil Biology and Biochemistry*, 42, 1222–1228. https://doi.org/10.1016/j.soilbio.2010.04.015

Sterner, R. W., & Elser, J. J. (2002). *Ecological stoichiometry: The biology of elements from molecules to the biosphere*. Princeton, NJ: Princeton University Press.

Tuomi, M., Laiho, R., Repo, A., & Liski, J. (2011). Wood decomposition model for boreal forests. *Ecological Modelling*, 222, 709–718. https://doi.org/10.1016/j.ecolmodel.2010.10.025

Valentin, L., Rajala, T., Peltoniemi, M., Heinonsalo, J., Pennanen, T., & Makipaa, R. (2014). Loss of diversity in wood-inhabiting fungal communities affects decomposition activity in Norway spruce wood. *Frontiers in Microbiology*, 5, 230. https://doi.org/10.3389/fmicb.2014.00230

Valmaseda, M., Almendros, G., & Martínez, A. T. (1990). Substrate-dependent degradation patterns in the decay of wheat straw and beech wood by ligninolytic fungi. *Applied Microbiology and Biotechnology*, 33, 481–484. https://doi.org/10.1007/BF00176671

Wang, C., Bond-Lamberty, B., & Gower, S. T. (2002). Environmental controls on carbon dioxide flux from black spruce coarse woody debris. *Ecosystems Ecology*, 132, 374–381. https://doi.org/10.1007/s00442-002-0987-4

Weedon, J. T., Cornwell, W. K., Cornelissen, J. H. C., Zanne, A. E., Wirth, C., & Coomes, D. A. (2009). Global meta-analysis of wood decomposition rates: A role for trait variation among tree species? *Ecology Letters*, 12, 45–56.

Weißhaupt, P., Pritzkow, W., & Noll, M. (2011). Nitrogen metabolism of wood decomposing basidiomycetes and their interaction with diazotrophs as revealed by IRMS. *International Journal of Mass Spectrometry*, 307, 225–231. https://doi.org/10.1016/j.ijms.2010.12.011

Welter, J. R., Benstead, J. P., Cross, W. F., Hood, J. M., Huryn, A. D., Johnson, P. W., & Williamson, T. J. (2015). Does N_2 fixation amplify the temperature dependence of ecosystem metabolism? *Ecology*, 96, 603–610.

Wu, J., Zhang, X., Wang, H., Sun, J., & Guan, D. (2010). Respiration of downed logs in an old-growth temperate forest in north-eastern

China. *Scandinavian Journal of Forest Research*, *25*, 500–506. https://doi.org/10.1080/02827581.2010.524166

Yang, C., Schaefer, D. A., Liu, W., Popescu, V. D., Yang, C., Wang, X., … Yu, D. W. (2016). Higher fungal diversity is correlated with lower CO_2 emissions from dead wood in a natural forest. *Scientific Reports*, *6*, 31066. https://doi.org/10.1038/srep31066

SUPPORTING INFORMATION

Additional supporting information may be found online in the Supporting Information section at the end of the article.